Estimation of spin-diffusion length from the magnitude of spin-current absorption: Multiterminal ferromagnetic/nonferromagnetic hybrid structures

T. Kimura,[1,2,3,*] J. Hamrle,[2,3] and Y. Otani[1,2,3]
[1]*Institute for Solid State Physics, University of Tokyo 5-1-5 Kashiwanoha, Kashiwa, Chiba 277-8581, Japan*
[2]*RIKEN FRS, 2-1 Hirosawa, Wako, Saitama 351-0198, Japan*
[3]*CREST, JST, Honcho 4-1-8, Kawaguchi, Saitama, 332-0012, Japan*
(Received 25 February 2005; revised manuscript received 31 May 2005; published 25 July 2005)

We demonstrate the method to calculate the spatial distributions of the spin current and accumulation in the multiterminal ferromagnetic/nonmagnetic hybrid structure using an approximate electrotransmission line. The analyses based on the obtained equation yield the results, in good agreement with the experimental ones. This implies that the method allows us to determine the spin diffusion length of an additionally connected electrically floating wire from the reduction of the spin signal.

DOI: 10.1103/PhysRevB.72.014461 PACS number(s): 75.70.Cn, 75.75.+a, 72.25.Ba, 72.25.Mk

I. INTRODUCTION

Spin-dependent electron transport phenomena in nanostructured ferromagnet (F)/normal metal (N) hybrid systems show intriguing characteristics in association with the spin transfer and accumulation. The devices based on spin transport phenomena have great advantages over the conventional electronic devices because of additional spin functionalities.[1] Therefore, understanding responsible physics on the spin diffusion process becomes essential to realize spin-electronic devices. Especially, electrical spin injection from F into N, semiconductor or superconductor, is an important technique for developing such devices.[2] When a spin-polarized current flows across the junction between F and N, the spin splitting in the chemical potential is induced in the N layer because of the sudden change in spin-dependent electrical conductivity.[3] This leads to the spin accumulation in the vicinity of the F/N interface. The injected spin can be flipped due to spin-orbit interaction, magnon, phonon scattering, etc. The length scale over which the traveling electron spin memorizes the initial direction is known as the spin diffusion length, an important measure to realize the efficient spin injection.

First electrical spin injection into N was demonstrated by Johnson and Silsbee using a single-crystalline Al bulk bar.[4] They found that the Al bar has a long spin diffusion length of a few hundred microns. However, the obtained output spin signal was quite small in the range of nano-Ohms due to large sample dimensions. The current perpendicular to plane (CPP) giant magnetoresistance measurements in magnetic multilayers of alternating F and N layers enable us to perform a more detailed study on the spin-diffusion process in the N layer because the relevant scale of the spin-diffusion length can be controlled by the spacer thickness.[5] This technique is suitable for the N layer with magnetic or even nonmagnetic impurities which reduce the spin diffusion length dramatically.[6] However, for Ns in which long spin diffusion lengths are expected, the precise estimation of the spin diffusion length is unattainable because of the difficulty in preparing a CPP device with the thickness of the N spacer as thick as the spin diffusion length. On the contrary, a planar mesoscopic spin-valve device is suitable to study the spin-dependent electron transport of the material that has long spin diffusion length. Recently, Jedema *et al.* succeeded in detecting the clear spin signal in the lateral structure, even at room temperature, by using nonlocal spin-valve (NLSV) measurements similar to the Johonson's potentiometric method.[7] In order to detect clear spin signals in the NLSV measurements, the spacing between the F injector and detector should be shorter than the spin-diffusion length of the material. This means that, for the Ns with spin diffusion length of subhundred nanometers, the NLSV technique cannot be applied because of the technical limit of device fabrication. We have experimentally demonstrated that in such lateral structures an additional floating probe that does not carry the charge current, affects the spin transport when the probe is located within the spin diffusion length from the spin injector.[8] In this article, we further extend the experiment for quantitative estimation of the spin-diffusion length using the spin absorption effect. (i.e., spin sink)

II. BASIC EQUATIONS

The continuous charge current I_C in the F subsection provides the spin current $I_S=\alpha_F I_C$, with α_F of the spin polarization in the F subsection. When the spin current flows across the F/N junction, the spin splitting in the chemical potential is induced in both F and N subsections, as shown in Fig. 1(a). Here, we divide the spin splitting chemical potential into two components. One is the voltage drop due to the charge current with the Ohmic resistance in each layer

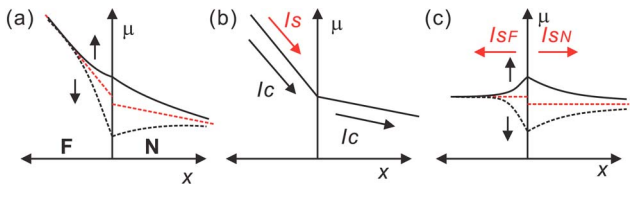

FIG. 1. (Color online) (a) Schematic illustrations of the spin splitting chemical potential induced by spin injection in the F/N junciton. (b) A component of the voltage drop due to the Ohmic resistance and (c) that of the spin splitting without charge current.

shown in Fig. 1(b). In this case, the distribution of the chemical potential is obtained by considering the conventional electrical circuit consisting of a series junction with two different resistances. A constant spin current I_S is induced by the continuous charge current in the F subsection. However, no spin current exists in the N subsection. The other one is the spin-dependent chemical potential without the contribution of Ohmic-resistance voltage drop, as shown in Fig. 1(c), where spin currents are generated both in the N and F layers. Since the source of the induced spin currents I_S is originated from the charge current of the F layer, the relation $I_S=I_{SF}+I_{SN}$ is satisfied at the interface. Here I_{SF} and I_{SN} are, respectively, the spin currents in the F and N subsections induced by the spin splitting of the chemical potential. Thus, the F/N junction with the charge current I_C acts as a spin-current source with the magnitude of $\alpha_F I_C$.

We consider the spin-splitting component of the chemical potential in which there is no charge current. The essential features for the spin-current and spin-accumulation distributions in the diffusive regime are described by the spin-dependent Boltzmann equation.[9] In general, from the one-dimensional diffusion equation, the induced spin-splitting voltage $\Delta V_S=\Delta\mu/e=(\mu_\uparrow-\mu_\downarrow)/e$, where $\mu_\uparrow$ and $\mu_\downarrow$ are the chemical potential of the up- and down-spins, respectively, is given by

$$\Delta V_S = V_+ e^{-x/\lambda} + V_- e^{x/\lambda}. \tag{1}$$

Here λ is the spin diffusion length. In the N layer, using the spin-dependent Ohmic law $I_{\uparrow,\downarrow}=(-\sigma_N S/2)\partial V_{\uparrow,\downarrow}/\partial x$, the spin current $I_{SN}=I_\uparrow-I_\downarrow$ is calculated as

$$I_{SN} = \frac{\sigma_N S_N}{2\lambda_N}(V_+ e^{-x/\lambda_N} - V_- e^{x/\lambda_N}) = \frac{1}{R_{SN}}(V_+ e^{-x/\lambda_N} - V_- e^{x/\lambda_N}), \tag{2}$$

where, S_N, σ_N, and λ_N are the cross-sectional area, the conductivity, and the spin diffusion length of the N subsection, respectively. The spin resistance R_{SN} is a measure of the difficulty for spin mixing and is defined as $2\lambda_N/(\sigma_N S_N)$. The situation described by Eqs. (1) and (2) is equivalent to the electrical transmission line of the characteristic impedance R_{SN} with the attenuation constant $1/\lambda_N$.[10]

We can also obtain the similar relation for the F layer. In the F subsection, the spin current I_{SF} is given by

$$I_{SF} = \frac{\sigma_F S_F}{2}\left((1+\alpha_F)\frac{\partial V_\uparrow}{\partial x} - (1-\alpha_F)\frac{\partial V_\downarrow}{\partial x}\right) \tag{3}$$

$$= \frac{\sigma_F S_F}{2}\left(\frac{\partial \Delta V_S}{\partial x} + \alpha_F\left(\frac{\partial V_\uparrow}{\partial x} + \frac{\partial V_\downarrow}{\partial x}\right)\right), \tag{4}$$

where S_F and σ_F are the cross-sectional area and the conductivity in the F subsection, respectively. Since there is no charge current, the relation $\alpha_F \partial \Delta V_S/\partial x = -(\partial V_\uparrow/\partial x + \partial V_\downarrow/\partial x)$ is satisfied. Therefore, the spin current I_{SF} in the F layer is given by

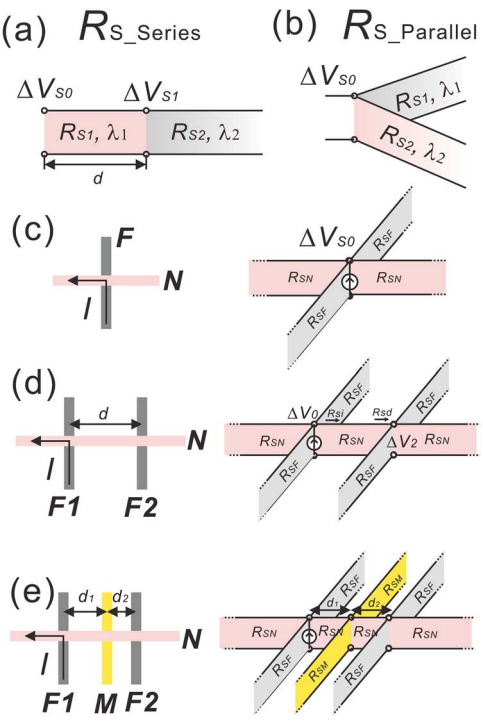

FIG. 2. (Color online) (a) Schematic illustrations of junction connected in series (a) and in parallel (b). With different characteristic spin resistances The distribution of the spin current and spin splitting can be similarly treated as an electrical transmission line. Schematic illustrations of (c) a single cross F/N junction with the equivalent circuit for the transmission calculation, (d) that of a double F/N junction, and (e) that of triple junction.

$$I_{SF} = \frac{(1-\alpha_F^2)\sigma_F S_F}{2\lambda_F}(V_+ e^{-x/\lambda_F} - V_- e^{x/\lambda_F}) = \frac{1}{R_{SF}}(V_+ e^{-x/\lambda_F} - V_- e^{x/\lambda_F}), \tag{5}$$

where λ_F is the spin diffusion length in the F subsection. Thus, in the F subsection, R_{SF} is given by $[1/(1-\alpha_F^2)] \times [2\lambda/(\sigma_F S_F)]$ instead of $2\lambda_N/(\sigma_N S_F)$. Equations (2) and (5) mean that the characteristic spin resistance over the spin-diffusion length is comparable to the characteristic impedance for the spin current and spin-splitting voltage.

Using these relations, we can simplify the calculation of the spatial distributions of spin current and accumulation in complex multiterminal F/N hybrid structures consisting of different characteristic spin resistances. We will show that the characteristic spin resistance R_S is an important measure to design the spin-dependent-transport property of the system.

First, we consider a cascaded transmission line of two different characteristic spin resistances, as shown in Fig. 2(a). Here, the first and second subsections have the characteristic resistance R_{S1} with the spin-diffusion length λ_1 and the characteristic resistance R_{S2} with the spin diffusion length λ_2, respectively. The length of the first subsection is d and the second subsection extends to infinity. The basic equations $\Delta V_{Si}(x)=V_{i+}e^{-x/\lambda_i}+V_{i-}e^{x/\lambda_i}$ and $I_{Si}(x)=(V_{i+}e^{-x/\lambda_i}$

$-V_{i-}e^{x/\lambda_i})/R_{Si}$ are valid for each subsection. In the second line, the coefficient V_{2-} of e^{x/λ_2} is zero because of its infinite length. Therefore, we obtain $\Delta V_{S2}(x)=V_{2+}e^{-x/\lambda_2}$ and $I_{S2}(x)=\Delta V_{S2}(x)/R_{S2}$. This relation and the continuities of I_S and ΔV_S at the junction yield $V_{1+}=e^{d/\lambda}V_{2+}(R_{S1}+R_{S2})/2R_{S2}$ and $V_{1-}=e^{-d/\lambda}V_{2+}(R_{S2}-R_{S1})/2R_{S2}$. We should note that the situations where $V_{1-}>0$ and $V_{1-}<0$, respectively, correspond to the spin-current absorption into the second line and the reflection from it due to the resistance mismatch at the boundary. We then define the transmission coefficient T as the ratio of the spin splitting voltage V_{S1} at the junction to the voltage V_{S0} at the input terminal. The transmission coefficient $T \equiv \Delta V_{S1}/\Delta V_{S0}$ is given by

$$T = \frac{R_{S2}}{R_{S1}\sinh(d/\lambda_1) + R_{S2}\cosh(d/\lambda_1)} = \frac{Q}{\sinh(d/\lambda_1) + Q\cosh(d/\lambda_1)}, \tag{6}$$

where Q is the ratio R_{S2}/R_{S1}. Defining the input spin resistance as $\Delta V_{S0}/I_{S0}$, where I_{S0} is the spin current at the input terminal, we obtain the input spin resistance in the series connection $R_{S\ series}$ as

$$R_{S\ series} = \frac{R_{S1}\sinh(d/\lambda_1) + R_{S2}\cosh(d/\lambda_1)}{R_{S1}\cosh(d/\lambda_1) + R_{S2}\sinh(d/\lambda_1)}R_{S1} = \frac{\sinh(d/\lambda_1) + Q\cosh(d/\lambda_1)}{\cosh(d/\lambda_1) + Q\sinh(d/\lambda_1)}R_{S1}. \tag{7}$$

The input spin resistance $R_{S\ parallel}$ in a parallel connection shown in Fig. 2(b) is also calculated as

$$R_{S\ parallel} = \frac{R_{S1}R_{S2}}{R_{S1}+R_{S2}} = \frac{R_{S2}}{1+Q}. \tag{8}$$

The previous basic equations can be applied for calculating the characteristics in multiterminal spin-transport systems.

In the above calculation, we assume a transparent interface between the different subsections with zero resistance. This assumption is justified only in limited materials. However, in this article, we treat Cu/Py and Cu/Au interfaces. These interfaces are known to have small resistance compared with other interfaces such as Cu/Pd and Cu/Pt.[5,6,11] Therefore, we neglected the interface resistance.

III. RESULTS AND DISCUSSIONS

A. Single junction

We now consider a single F/N cross junction with the charge current I_C flowing across the F/N interface, as shown in Fig. 2(c). As mentioned previously, the charge current across the junction plays a role of the spin current source with the magnitude of $\alpha_F I_C$. The induced spin current diffuses into each subsection according to the magnitude of characteristic spin resistance. This can be described as the parallel spin resistance circuit consisting of two F and two N subsections shown in Fig. 2(c). We can now calculate the induced spin-splitting voltage V_{S0} at the interface as

$$\Delta V_{S0} = \alpha_F I_C \frac{R_{SF}R_{SN}}{2(R_{SF}+R_{SN})}. \tag{9}$$

The spin splitting decays exponentially over the spin diffusion length in each subsection.

B. Double junction

Unfortunately, we cannot experimentally determine the spin splitting of the chemical potential in the above single junction, although the spin splitting can be induced in the N subsection. When an additional F probe (F_2) is connected to the N subsection within the spin diffusion length from the spin-polarized current injector, as shown in Fig. 2(d), the voltage difference between the F_2 and N subsections can be detected as the boundary resistance caused by the spin splitting. Remarked here is that the spin-current and chemical-potential distributions are significantly affected by the additional wire. We discuss the double F/N junctions on the basis of the transmission model. In this case, the input spin resistance R_{Si} for the nonlocal lead consisting of the N and F layers changes from R_{SN}, resulting in the different spin-splitting voltage from the single junction. The R_{Si} can be calculated by considering a cascaded transmission line of R_{SN} and R_{Sd} with the junction at the position d. Here, R_{Sd} is the spin resistance from the detector junction and is given by

$$R_{Sd} = \frac{R_{SN}R_{SF}/2}{R_{SF}/2+R_{SN}} = \frac{R_{SF}}{2+Q}. \tag{10}$$

From Eq. (7), R_{Si} is deduced as

$$R_{Si} = \frac{R_{SN}\sinh(d/\lambda_N) + R_{Sd}\cosh(d/\lambda_N)}{R_{SN}\cosh(d/\lambda_N) + R_{Sd}\sinh(d/\lambda_N)}R_{SN} = R_{SN} - \frac{2\,R_{SN}}{1+e^{2d/\lambda_N}(1+2Q)}. \tag{11}$$

The total spin resistance of the device R_S is given as the parallel sum of R_N, two R_F, and R_{Si}:

$$R_S = \left(\frac{1}{R_{SN}} + \frac{2}{R_{SF}} + \frac{1}{R_{Si}}\right)^{-1} = \frac{QR_{SN}[e^{d/\lambda_N}Q + 2\sinh(d/\lambda_N)]}{2[e^{d/\lambda_N}Q(2+Q) + 2\sinh(d/\lambda_N)]}. \tag{12}$$

Also using Eq. (6), the transmission coefficient of the device T_2 corresponding to the ratio of the spin-splitting voltage between the injector and detector F/N interfaces can be calculated as

$$T_2 = \frac{R_{Sd}}{R_{SN}\sinh(d/\lambda_N) + R_{Sd}\cosh(d/\lambda_N)} = \frac{Q}{e^{d/\lambda_N}Q + 2\sinh(d/\lambda_N)}. \tag{13}$$

The induced spin-splitting voltage at the injector junction is given by $I_S R_S$. Then, the induced spin-splitting voltage ΔV_{S2} at the detector junction can be calculated by $\Delta V_{S2}=T_2 I_S R_S$. Since the NLSV signal ΔV_{N2} is given by $\alpha_F \Delta V_{S2}$,[12] we obtain

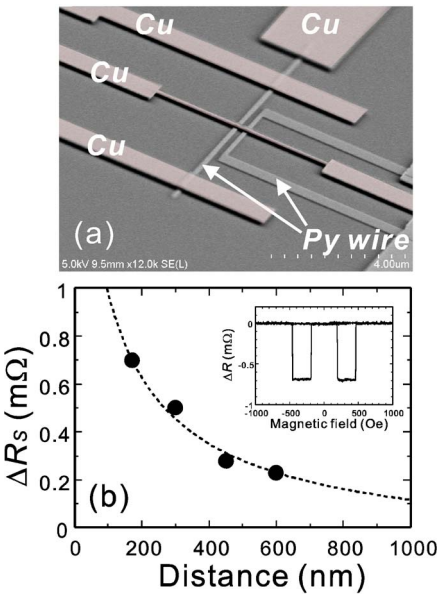

FIG. 3. (Color online) (a) SEM images of the typical lateral spin device consisting of the double Py/Cu junctions. (b) NLSV signal measured at room temperature as a function of the distance d between F injector and F detector. The inset of (b) is an obtained NLSV curve for the distance d=270 nm.

$$\Delta V_{\mathrm{N2}} = \frac{\alpha_F I_S Q^2 R_{\mathrm{SN}}}{2e^{d/\lambda_N}(2+Q) + 4\sinh(d/\lambda_N)}. \tag{14}$$

We experimentally demonstrate the precise estimation of the spin diffusion lengths of F and N strips and the spin polarization of F strips using Eq. (14). The lateral spin valves for this study consist of double Py/Cu junctions. Figure 3(a) shows a SEM image of the typical fabricated device. Here, the width of both Py and Cu strips is 100 nm and the thicknesses of Py and Cu strips are 30 and 80 nm, respectively. The resistivities of the Py and Cu strips are, respectively, 26.8 and 2.08 $\mu\Omega$ cm at room temperature. We vary the distance between the injector and detector junctions from 270 to 700 nm and measure the NLSV signal at room temperature as a function of the distance. In order to compare quantitatively Eq. (14) with the experimental spin signal, the cross sections S_{Cu} and S_{Py} have to be known to obtain the spin resistance of each strip. We thus have to carefully estimate the cross sections. From previous reports, λ_{Cu} is of the order of several hundred nanometers and λ_{Py} is a few nanometers.[7,13–15] Since the spin-current flows along the Cu strip over a few hundred of nanometers, the area S_{Cu} for estimating R_{Cu} should be given by the cross section of the Cu strip (100 nm$\times$80 nm). On the other hand, in the Py strip, the cross section is not appropriate for the area S_{Py} for R_{SPy} because the spin current diminishes in the vicinity of the junction. Therefore, for the Py strip S_{Py} should be the junction area 100 nm$\times$100 nm.[16]

A NLSV signal at a distance of 270 nm as a function of the external magnetic field parallel to the Py strip is shown in the inset of Fig. 3(b). We observe the clear spin-accumulation signal at room temperature. Figure 3(b) shows the NLSV signal as a function of the distance d. The obtained signal decreases monotonically with increasing the distance d due to the spin relaxation. This result is fitted to Eq. (14). As shown in Fig. 3(b), the fitted curve is in good agreement with the experimental results. From the fitting parameter, we obtain the spin-diffusion length of the Cu strip and that of the Py strip as 500 and 3 nm, respectively. And also, the polarization α_{Py} of the Py strip is determined as 0.25 at room temperature. Here, λ_{Cu}=500 nm is quite long compared with other reported values.[7,14] We notice that the resistivity of our Cu is rather smaller than that of the reported one. This supports the long spin diffusion length of our Cu strip. λ_{Py}=3 nm and α_{Py}=0.25 are reasonable although the values are slightly smaller than other group's values. This may be due to the rather higher resistivity of our Py than others. Using these values, we can calculate the characteristic spin resistance of each strip as R_{SCu}=2.60 Ω and R_{SPy} =0.34 Ω.

C. Triple junction

We extend the above formalism to a triple junction in Fig. 2(e). In this case, the output spin-splitting voltage induced between the F2 and N strip by the current injection from F1 is influenced by the M strip that absorbs the induced spin current. The middle strip has the spin resistance of R_{SM} with the spin diffusion length λ_{M}. The magnitude of the spin current and spin accumulation can be calculated by using the method explained above. From the calculation, the position of the middle wire was found not to affect the spin signal. Therefore, for simplicity we assume that the middle wire is located in the center between F1 and F2 strips that have the same spin resistances of R_{SF}. When the current is injected from F1, the NLSV voltage ΔV_{N3} at the junction of F2/N is given by

$$\Delta V_{\mathrm{N3}} = \frac{\alpha_F I_S Q^2 Q_{\mathrm{M}} R_{\mathrm{SN}}}{2\{-2(1+Q) + [2+Q(2+Q)(1+Q_{\mathrm{M}})]\cosh(d/\lambda_{\mathrm{N}}) + [2Q_{\mathrm{M}} + Q(2+Q)(1+Q_{\mathrm{M}})]\sinh(d/\lambda_{\mathrm{N}})\}}, \tag{15}$$

where Q and Q_{M} are, respectively, defined as $R_{\mathrm{SF}}/R_{\mathrm{SN}}$ and $R_{\mathrm{SM}}/R_{\mathrm{SN}}$. d is the distance between the injector and detector. $Q_{\mathrm{M}}=\infty$ corresponds the case without an M strip.

The lateral spin valves consisting of the triple junctions are then prepared with changing the material for the M strip. We know the spin resistances of Py and Cu strips from the

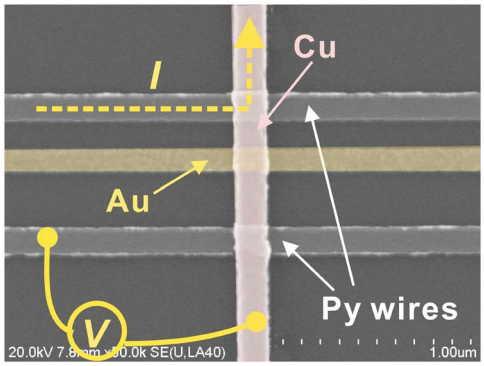

FIG. 4. (Color online) SEM images of the typical lateral spin device consisting of the double Py/Cu junctions and the middle Au/Cu junction.

previous double-junction experiment. Therefore, the Py and Cu wires were used as an F and N strip, respectively. Cu, Py, and Au are chosen as the material of the middle strip. The width and thickness of each strip are the same as those of the double junction. Figure 4 shows a fabricated lateral spin valve of the triple junctions with a Au M strip. The distance d between injector and detector Py/Cu junctions is 650 nm. The M wire is located at an intermediate position between the injector and detector. The NLSV is measured with the probe configuration in Fig. 4(b). Using the spin resistances $R_{SCu}=2.60\ \Omega$, $R_{SPy}=0.34\ \Omega$, and Eq. (16), we obtain the following equation between the detected spin signal R_{NLSV} and R_{SM}:

$$R_{SM}[\Omega] = \frac{7.02R_{NLSV}(\mathrm{m}\Omega)}{1.27 - 4.41R_{NLSV}(\mathrm{m}\Omega)}. \qquad (16)$$

Figure 5(a) shows the NLSV signal of the device with the Cu M strip. We obtained the spin signal of 0.18 mΩ smaller than the value of 0.27 mΩ obtained without the middle wire. This is because a small amount of the spin current is absorbed into the middle Cu strip. Figure 5(b) shows the NLSV signal of the device with the Py M strip. Here the difference in the switching field between Figs. 5(a) and 5(b) due to the shape of both injector- and detector-F strips to the large pad.[8] The spin signal exhibits a drastic reduction to 0.05 mΩ, much smaller than that without the M strip. This is also due to the spin-current absorption into the Py M strip. However, because of the small spin resistance of the Py strip, the spin current is preferably absorbed into the Py M strip, resulting in a much smaller spin signal in the NLSV measurement. Figure 5(c) shows the NLSV signal of the device with the Au M strip. The obtained spin signal is 0.08 mΩ and shows the large reduction of the spin signal similar to that of the M Py strip. This implies that the Au wire has smaller spin resistance.

Figure 6 shows the spin resistance of the M strip R_{SM} as a function of R_{NLSV} based on Eq. (16). From the equation, we obtain the spin resistances of the Cu, Au, and Py strips as 2.67, 0.62, and 0.33 Ω. The experimental values for the Py and Cu M strips are quantitatively in good agreement with the ones obtained from the double junction experiment. This indicates that Eq. (16) is valid for estimating the spin resistance of the M strip. For the Au strip, since the resistivity of the Au strip is 5.24 $\mu\Omega$ cm, we obtain the spin-diffusion length of the Au strip as 60 nm. This is in good agreement with the other reports[15] and proves that the Au strip has short spin-diffusion length due to the strong spin-orbit interaction.[17] Thus, using this method, we can estimate the characteristic spin resistance and spin diffusion length of the material.

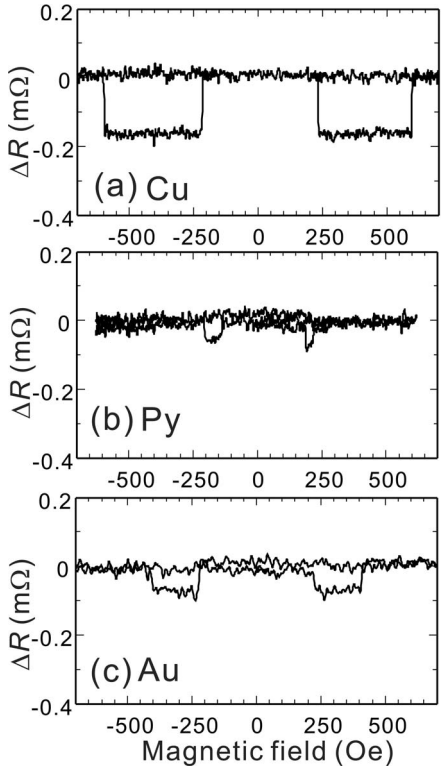

FIG. 5. (a) Nonlocal spin-valve curve with the Cu middle wire, (b) that with the Py middle wire, and (c) with the Au middle wire.

IV. CONCLUSION

We have shown the calculation of the spin-current and

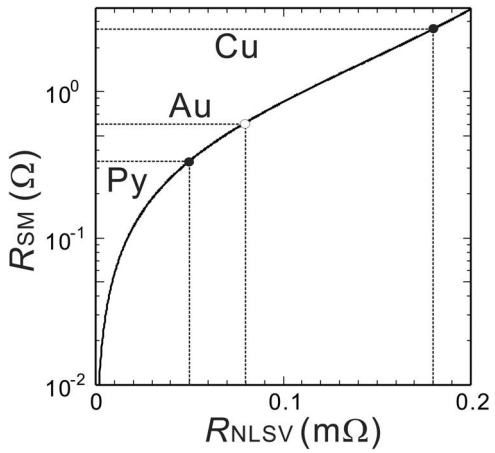

FIG. 6. Calculated spin resistance as a function of the obtained nonlocal spin signal R_{NLSV}.

spin-splitting-voltage distributions in the multiterminal F/N hybrid structure by introducing the characteristic spin resistance and similarly treating the system as an electrotransmission line. The analyses based on this method give the values in good agreement with the experimental results. The spin diffusion length of our Cu strip was found to be 500 nm quite long at room temperature. The model is extended to the triple F/N junctions consisting of a conventional lateral spin valve with an additionally connected floating strip that is located in between the injector and detector. When the spin resistance of the additional strip is much smaller than that of the N strip, the spin currents tend to flow into the additional strip to be relaxed. We also emphasize that, using the absorption effect, the spin-diffusion length of the additional strip can be estimated quantitatively from the reduction of the spin signal in the NLSV measurement. The situation of the present experiment may be directly compared with the spin pumping effect observed in magnetic multilayers.[18]

*Electronic address: kimura@issp.u-tokyo.ac.jp

[1] A. Brataas, Y. Tserkovnyak, G. E. W. Bauer, and B. I. Halperin Phys. Rev. B **66** 060404(R) (2002); G. E. W. Bauer, A. Brataas, Y. Tserkovnyak, and B. J. van Wees, Appl. Phys. Lett. **82**, 3928 (2003).

[2] G. Schmidt, D. Ferrand, L. W. Molenkamp, A. T. Filip, and B. J. van Wees, Phys. Rev. B **62**, R4790 (2000).

[3] P. C. van Son, H. van Kempen, and P. Wyder, Phys. Rev. Lett. **58**, 2271 (1987).

[4] M. Johnson and R. H. Silsbee, Phys. Rev. Lett. **55**, 1790 (1985).

[5] W. P. Pratt, Jr., S.-F. Lee, J. M. Slaughter, R. Loloee, P. A. Schroeder, and J. Bass, Phys. Rev. Lett. **66**, 3060 (1991).

[6] Q. Yang, P. Holody, S.-F. Lee, L. L. Henry, R. Loloee, P. A. Schroeder, W. P. Pratt, Jr., and J. Bass Phys. Rev. Lett. **72**, 3274 (1994).

[7] F. J. Jedema, A. T. Filip, and B. J. van Wees, Nature (London) **410**, 345 (2001); F. J. Jedema, M. S. Nijboer, A. T. Filip, and B. J. van Wees, Phys. Rev. B **67**, 085319 (2003).

[8] T. Kimura, J. Hamrle, Y. Otani, K. Tsukagoshi, and Y. Aoyagi, Appl. Phys. Lett. **85**, 3795 (2004).

[9] T. Valet and A. Fert, Phys. Rev. B **48**, 7099 (1993).

[10] S. Ramo, J. R. Winnery, and T. V. Duzer, *Fields and Waves in Communication Electronics*, 3rd ed. (Wiley, New York, 19XX), pp.

[11] H. Kurt, Wen-C. Chiang, C. Ritz, K. Eid, W. P. Pratt, Jr., and J. Bass, J. Appl. Phys. **93**, 7918 (2003)

[12] T. Kimura, J. Hamrle, Y. Otani, K. Tsukagoshi, and Y. Aoyagi, Appl. Phys. Lett. **85**, 3501 (2004).

[13] S. Dubois, L. Piraux, J. M. George, K. Ounadjela, J. L. Duvail, and A. Fert, Phys. Rev. B **60**, 477 (1999).

[14] F. J. Albert, N. C. Emley, E. B. Myers, D. C. Ralph, and R. A. Buhrman, Phys. Rev. Lett. **89**, 226802 (2002).

[15] W-C. Chiang, C. Ritz, K. Eid, R. Loloee, W. P. Pratt, and J. Bass, Phys. Rev. B **69**, 184405 (2004).

[16] S. Takahashi and S. Maekawa, Phys. Rev. B **67**, 052409 (2003).

[17] B. Pannetier, J. Chaussy, R. Rammal, and P. Gandit, Phys. Rev. B **31**, 3209 (1985).

[18] Y. Tserkovnyak, A. Brataas, and G. E. W. Bauer, Phys. Rev. B **66**, 224403 (2002).